Clustering and fluidization in a one-dimensional granular system: Molecular dynamics and direct-simulation Monte Carlo method

José Miguel Pasini* and Patricio Cordero†

Departamento de Física, Facultad de Ciencias Físicas y Matemáticas, Universidad de Chile, Santiago, Chile

We study a one-dimensional granular gas of pointlike particles not subject to gravity between two walls at temperatures T_{left} and T_{right}. The system exhibits two distinct regimes, depending on the normalized temperature difference $\Delta = (T_{\text{right}} - T_{\text{left}})/(T_{\text{right}} + T_{\text{left}})$: one completely fluidized and one in which a cluster coexists with the fluidized gas. When Δ is above a certain threshold, cluster formation is fully inhibited, obtaining a completely fluidized state. The mechanism that produces these two phases is explained. In the fluidized state the velocity distribution function exhibits peculiar non-Gaussian features. For this state, comparison between integration of the Boltzmann equation using the direct-simulation Monte Carlo method and results stemming from microscopic Newtonian molecular dynamics gives good coincidence, establishing that the non-Gaussian features observed do not arise from the onset of correlations.

PACS number(s): 45.70.−n, 81.05.Rm, 05.20.Dd, 05.10.Ln

I. INTRODUCTION

Granular systems have been extensively studied due both to the theoretical challenges they present (for a recent review, see Ref. [1]) and to the applications of industrial importance that spring from the rich phenomena they exhibit (see Refs. [2] and [3] and references therein). These systems are characterized by an energy loss in collisions. This loss is at the base of many interesting phenomena, such as inelastic collapse [4,5], where the particles collide infinitely often in finite time, and clustering (for a sample of theoretical, simulational, and experimental approaches see Refs. [6–9]). Different methods for keeping the system from collapsing have been devised, such as subjecting the particles to Brownian forces [10,11], and forcing through the boundaries by putting the system in a box with one or more thermal-like walls (see, for example, Refs. [12–18]). This work focuses on the latter method.

Being one of the simplest types of forcing, several authors [12,13,15–17,19] have studied a one-dimensional system in a box with one or two heated (stochastic) walls. Of these, Refs. [12,13,15] and [16] study cluster formation, although Refs. [15] and [16] are not strictly one dimensional.

This article studies a quasielastic one-dimensional system not subject to gravity between two thermalizing walls. We focus on two control parameters: the total inelasticity parameter $qN \equiv N(1-r)/2$, where N is the number of particles and r is the restitution coefficient, and the externally imposed temperature gradient. The parameter qN has been shown to be relevant for the quasielastic system [13,17,19–21]. By varying these parameters we determine the region in parameter space where clustering is fully inhibited, obtaining a fluidized state. We present a singular feature of the distribution function for the clustering regime, and then study how this feature is modified for the fluidized state.

In Ref. [12] the authors study a one-dimensional system of pointlike particles between an elastic and a heated wall. They emphasize that a cluster inevitably forms away from the heated wall, regardless of how elastic the system is (as long as it is not perfectly elastic). They also study the same system, but with both walls expelling the particles with a fixed velocity. In this case they find that the cluster forms away from the walls and roams slowly about the system, with two groups of fast particles connecting the cluster with the ''heated'' walls.

In Ref. [13] the same system is studied for different types of boundary conditions at the heated wall. The stochastic boundary condition studied has the form of a power of the velocity times the ''thermal'' condition (the one that produces a Maxwell-Boltzmann distribution in the elastic case). The authors show that when the power that multiplies the thermal condition is positive the test-particle equation (derived from the Boltzmann equation) has a steady-state solution. Thus the thermal case does not have a steady state and develops a cluster away from the heated wall. The mechanism for the growth of the cluster is explained and verified numerically.

In Ref. [15] a similar system is studied: a long thin pipe of inelastic hard disks with heated walls (at the same temperature) at the ends of the pipe and periodic side walls. The pipe is thin enough for the particle order to be preserved. The probability distribution for the distance between the central particles is studied. This distribution gives a markedly denser system near the center than in the elastic case, although the limit to the elastic case is smooth, unlike the strictly one-dimensional case of Refs. [12] and [13]. In Ref. [16] the same author studies the velocity correlations that this system develops as inelasticity is increased, showing that a consistent description must take these correlations into account.

In this paper we revisit the strictly one-dimensional system of N pointlike particles interacting via collisions that conserve momentum but dissipate kinetic energy. To fix notation, the particle velocities after a collision are given by

$$c_1' = qc_1 + (1-q)c_2, \quad c_2' = (1-q)c_1 + qc_2, \qquad (1)$$

---

*Electronic address: jpasinik@cec.uchile.cl

†URL: http://www.cec.uchile.cl/cinetica/

where c_i is the velocity of particle i before a collision, and $q=(1-r)/2$, r being the restitution coefficient. For the elastic case ($r=1$) the particles simply exchange velocities. Since the particles are pointlike, the system is then indistinguishable from a system in which the particles do not interact.

This one-dimensional system is interesting because dissipation is the first order correction to a free gas. Besides, results for the one-dimensional system have been found to have unexpected relevance for higher-dimensional problems. For example, in two-dimensions the particles involved in inelastic collapse lie roughly on a line [5]. Also, the dissipation-induced temperature gradients calculated in Ref. [17] for the one-dimensional case inspired the authors to look for dissipation-induced Rayleigh-Bénard-like convection for a two-dimensional system without an externally imposed temperature gradient [18].

For a system with one thermal wall and open on the other side, under the influence of gravity, the quasielastic system may be kept fluidized [17,19]: any cluster that starts to form is forced against the thermal wall, where it evaporates. In [17] the test-particle equation [12,13,20]—which is the one-dimensional (1D) Boltzmann equation where the limit $N \rightarrow \infty$ is taken, but keeping qN fixed—is successfully applied, with close matching of theory and simulations even at the level of the distribution function.

The one-dimensional system under study is left to evolve between two thermal walls at temperatures T_{left} and T_{right}, with $T_{\text{left}} \lesssim T_{\text{right}}$. We define the parameter

$$\Delta \equiv \frac{T_{\text{right}} - T_{\text{left}}}{T_{\text{right}} + T_{\text{left}}} \qquad (2)$$

to quantify how far from the symmetrical case is the system. Under the same conditions, an elastic system has a perfectly bimodal velocity distribution with global homogeneous temperature equal to $\sqrt{T_{\text{left}} T_{\text{right}}}$. For the sake of comparison, we simulate systems with $\sqrt{T_{\text{left}} T_{\text{right}}} = 1$. Here $\Delta = 0$ represents a symmetrical setting, while $\Delta = 1$ represents an infinitely strong temperature gradient.

As in Ref. [12], for $\Delta = 0$ a cluster unavoidably forms away from the thermal walls. After forming, the cluster performs an apparently random walk about the center, growing in size (and therefore mass) while the rest of the system grows more rarefied. With the decrease in density of the surrounding gas and the increased inertia of the cluster, an eventual collision with one of the walls is to be expected. When this happens part of the cluster evaporates, and what is left of it is expelled from the wall (see Fig. 1), thus restarting the growth process. Thus not only is the system highly clumped, but also in a nonsteady state. Nevertheless, the gas that is far from the random-walk zone has a well-defined time average for the distribution function, as is seen in Fig. 2. A noteworthy feature of this distribution is that it exhibits apparently singular behavior for slow velocities.

Setting $\Delta \neq 0$ the symmetry of the system is broken. For $\Delta \ll 1$ the cluster performs a slightly asymmetric random walk, spending more time near the colder wall, and therefore colliding more often with it. Thus the cluster cannot grow as
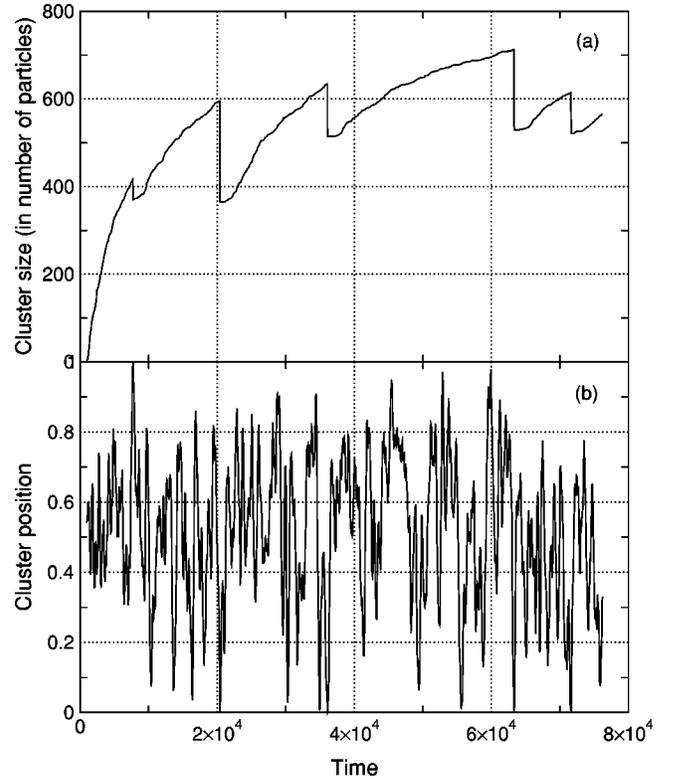
FIG. 1. (a) Time evolution of the number of particles inside the cluster for a system of $N=1000$ particles between two walls at the same temperature for $qN=0.01$. Note the plateau after each fall. (b) Trajectory of the cluster for the same time interval. The walls are placed at $x=0$ and 1. The temperature at the walls is unity, and thus a unit of time measures how long it takes for a particle with the thermal speed to cross the system.

much as it did in the symmetric case before colliding with a wall. By increasing Δ the cluster-wall collision frequency grows, even obtaining short "windows" in which the cluster completely evaporates.

By further increasing Δ these windows grow larger until a point is reached where no cluster forms. In this fashion a totally fluidized state is achieved, which may be tractable with the dissipative Boltzmann equation. However, the distribution function obtained from the molecular dynamics (MD) simulations exhibits a peculiar non-Gaussian feature for slow velocities. This feature is a smoothed version of the apparent singularity of the symmetric case.

To discern whether this non-Gaussian feature is due to correlations or is present before they settle in, we compared Newtonian molecular dynamics results with those obtained through the direct-simulation Monte Carlo method (DSMC), which neglects correlations. The density profiles show a denser system towards the colder wall, although when the system is sufficiently far from the onset of clustering the density has a maximum slightly away from the wall. The profiles and the velocity distribution function obtained from DSMC are practically identical to the ones obtained from molecular dynamics, except when the system is very close to the onset of clustering. At this point the DSMC velocity distribution shows a slight (but systematic) overpopulation of
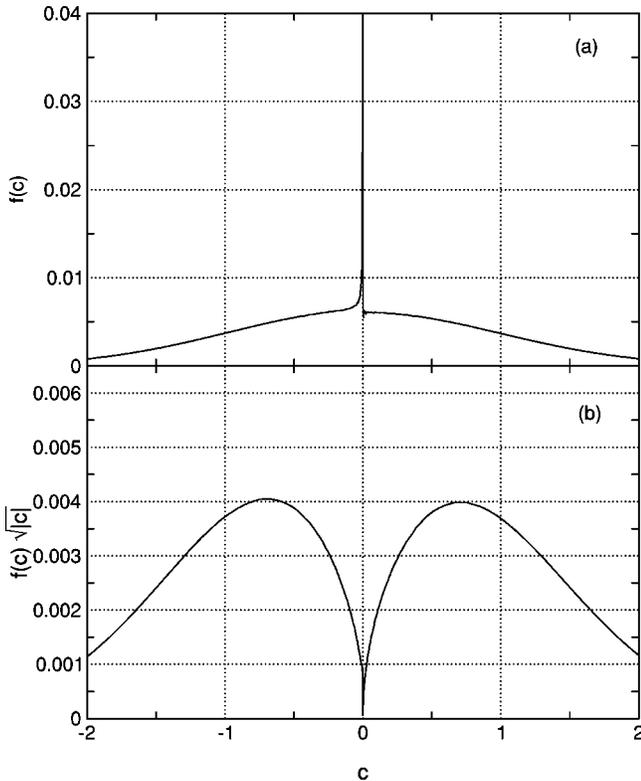
FIG. 2. (a) Velocity distribution function at the left wall for the system referred to in Fig. 1. The distribution for particles reaching the wall ($c<0$) exhibits a sharp peak. (b) The same distribution multiplied by $\sqrt{|c|}$ to show that the peak behaves like $|c|^{-1/2}$. The microscopic velocity c is measured in units of the thermal speed.

slow particles, compared to the MD results, and a corresponding relative increase in the density at the colder wall. Both the MD and DSMC results exhibit the sharp non-Gaussian feature even far from the clustering regime, where both descriptions coincide. This will lead us to conclude that this feature does not arise from correlations.

II. SIMULATION METHOD

We simulate the system through event-driven molecular dynamics [22] and through direct-simulation Monte Carlo [23]. The direct-simulation Monte Carlo procedures use the null-collision technique [24] where, overestimating the collision frequency (using the maximum relative velocity within a cell), the number of collisions to be *attempted* is calculated through a Poisson process. In the next step the collisions are attempted, choosing at random two particles within the cell, and making them collide with a probability proportional to their relative velocity. Most of the molecular dynamics and DSMC simulations were done with $N=1000$ particles.

In the MD simulations we detect clusters using a geometric criterion: we consider chains of particles that are nearer than a critical distance (in our case 10^{-6} and 10^{-5}, to be certain that the conclusions are independent of the choice). The system length is one, and with a thousand particles the mean distance between neighbors for a homogeneous system is 10^{-3}. Thus we detect particles that are uncommonly near

by three orders of magnitude. We discard chains of length three or less, since they may be random encounters. Measuring the *total* length of the cluster we have found that on average it is of the order of 10^{-5}; thus the choice of 10^{-5} as link-link distance is much larger than the true distance between them.

As already stated, the boundary conditions are such that the (homogeneous) temperature of the corresponding elastic system (equal to $\sqrt{T_{\text{left}}T_{\text{right}}}$) is 1.

III. RESULTS

A. Clustering regime

Figure 1 shows the nonsteady state of a granular system between two walls at the same temperature for $qN=0.01$. A cluster forms away from the walls, performing a random walk of varying amplitude. When the cluster reaches a wall, part of it evaporates, and the growth process begins anew.

As is usual for the quasielastic case, we relabel the particles when they collide. This enables us to visualize this system as a group of barely interacting particles passing through each other.

The picture for cluster evolution, as explained before, is the following: the cluster grows because the slowest particles, due to the asymmetry of the distribution function, drift towards the cluster [13]. As it grows, the density of the gas surrounding it decreases, with the consequent saturation in growth. Thus we have a ''Brownian particle'' of increasing mass moving in an increasingly rarefied medium. This ''particle'' will be increasingly less affected by the surrounding medium, until it can no longer be kept away from the walls.

The cluster moves several orders of magnitude slower than the thermal speed (three orders of magnitude in Fig. 1). Upon reaching a wall, the front liners strike the wall and are expelled by it much faster than the other cluster members. These particles pass through the cluster, transferring momentum to it, as described in Ref. [12]. Thus these fast particles push the cluster away from the wall, where it can absorb particles again. The fast particles, however, no longer belong to the cluster.

Since the slowest particles in the gas are the ones that will be absorbed by the cluster [13], it is the number of slow particles in the gas that will determine the cluster's growth rate. After the cluster strikes a wall, the expelled particles will be fast particles, and they will not contribute to the growth of the cluster during the time it takes for the gas to cool down again: the only particles available for absorption are the ones that were available before the cluster-wall collision. This explains why the cluster keeps growing at approximately the same rate it did before the collision. After the gas has cooled down, the growth rate returns to its normal value. This is the end of the plateau seen in Fig. 1 after each cluster-wall collision.

To quantify the evaporation process we proceed as in Refs. [1] and [12]: as soon as the first particle belonging to the cluster reaches a wall, it is expelled with a speed much higher than the cluster velocity; thus we may consider the ideal situation of a cluster of M particles at rest being stricken by a fast particle with velocity v (in this case v

≈ 1). After colliding with the first particle in the cluster, the new fast particle's speed will be $(1-q)$. Thus, after traversing the cluster, the fast particle's velocity will be $(1-q)^N$. Since momentum is conserved in collisions, the center of mass of the cluster will have acquired a speed of

$$v_{CM} = \frac{1-(1-q)^N}{N} = \frac{1-\left(1-\dfrac{qN}{N}\right)^N}{N}. \quad (3)$$

Considering the case $N \gg 1$ with fixed qN, as in Ref. [17], we may simplify this expression to

$$v_{CM} \approx \frac{1-e^{-qN}}{N}. \quad (4)$$

By further considering the case $qN \ll 1$ we get $v_{CM} \approx q$. In this limit, if the cluster reaches the wall with velocity v_0 and is expelled from it with velocity v_1, the number m of particles evaporated will satisfy $|v_1 - v_0| \approx mq$. For the situation shown in Fig. 1, v_0 and v_1 are typically of the order of 10^{-3} and $q = 10^{-5}$, hence the number of particles evaporated will be of the order of 10^2.

Even if the system is in a nonsteady state, the gas at the walls (far from the random-walk zone) has a well-defined time average for the distribution function. The distribution function at the left wall is shown in Fig. 2. There is an apparent singularity for slow velocities. The distribution is asymmetric as it should be, since the particles leaving the wall ($c > 0$) follow a Gaussian distribution. Figure 2 also shows the distribution multiplied by $\sqrt{|c|}$. Since the limit of $\sqrt{|c|}f$ for $c \to 0^-$ is finite and nonzero, we conclude that the distribution function exhibits a singularity that behaves like $|c|^{-1/2}$ for slow velocities.

As shown in Ref. [13], when $\Delta = 0$ (the symmetric case) the distribution shown in Fig. 2 is not a solution of the steady-state test-particle equation:

$$c\partial_x f(x,c,t) = qN\partial_c[f(x,c,t)M(x,c,t)], \quad (5)$$

where

$$M(x,c,t) = \int_{-\infty}^{\infty} f(x,c',t)(c-c')|c-c'|dc'. \quad (6)$$

To establish this, let us study the behavior for small c of a solution of this equation. Assume that, for small c, $f(x,c \approx 0) \approx f_0(x)c^{-\alpha}$, with $\alpha < 1$ in order to have a finite density in the vicinity of x. Furthermore, assume that $M(x,c \approx 0) \approx M_0(x)c^\beta$. Inserting this behavior in Eq. (5) we obtain

$$\partial_x f_0 \approx qNM_0 f_0(\beta - \alpha)c^{\beta-2}. \quad (7)$$

Thus, in order to keep f_0 (the amplitude of the singularity) finite, we must have either $\beta = \alpha$ or $\beta \geq 2$. Integrating the distribution of Fig. 2 we obtain $\beta = 1$. Since $\beta < 2$, we must have $\alpha = 1$. But this corresponds to a nonintegrable distribution, and therefore the distribution cannot be steady.
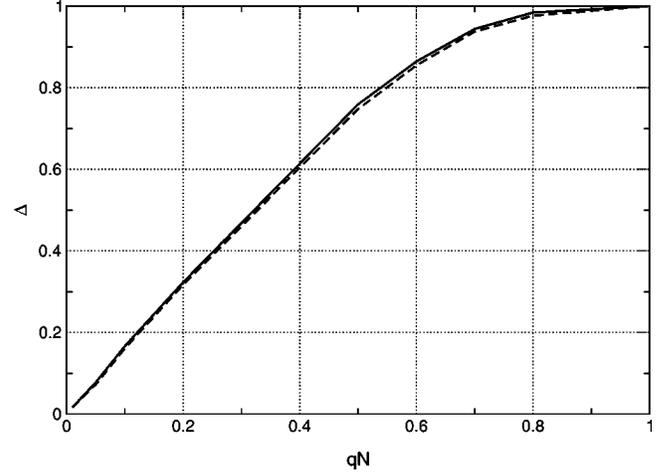
FIG. 3. Limiting values of $\Delta \equiv (T_{right} - T_{left})/(T_{right} + T_{left})$ as a function of qN for $N = 1000$. $\sqrt{T_{left}T_{right}} = 1$ throughout. The solid curve shows the lowest possible value Δ can take without detecting clusters. The dashed curve shows the largest possible value Δ can take with easy cluster detection. The small region between the curves represents a zone where clusters appear erratically.

B. Inhibition of cluster formation

Figure 3 shows the regions in (Δ, qN) space where clustering is inhibited for $N = 1000$. As is to be expected, as the inelasticity increases, a stronger temperature gradient is necessary to inhibit cluster formation.

To discern whether the non-Gaussian features of the velocity distribution function are derived from correlations in the system we compared results from MD simulations (full Newtonian dynamics) with results from DSMC simulations (no velocity correlations assumed). Figures 4 and 5 show this comparison for a case far from the clustering threshold ($\Delta = 0.6$ and $qN = 0.1$). The temperatures of the left and right walls are chosen so that the global temperature for the elastic case (equal to $\sqrt{T_{left}T_{right}}$) is 1. The curves match almost exactly.

At the level of the distribution function, the results also match closely. The peculiar non-Gaussian feature of the distribution function is clearly seen in Fig. 5. There is some slight mismatch near the peak.

For the fluidized case, since momentum is conserved and the system is stationary, the pressure is constant throughout the system. The number density and the granular temperature calculated here are related by $p = nT$ (T in energy units). Thus when the normalized density n/N varies little throughout the system $[n/N \approx 1 + \epsilon(x)]$, the normalized temperature is

$$\frac{T}{T_0} = \frac{p/n}{p/n_0} = \frac{n_0/N}{n/N} = \frac{1}{1+\epsilon(x)} \approx 1 - \epsilon(x), \quad (8)$$

thus obtaining the nearly symmetric profiles seen in Figs. 4 and 6.

Figures 6–8 compare the MD and DSMC results for cases near cluster formation. The non-Gaussian feature of the distribution function shows a systematic deviation for DSMC
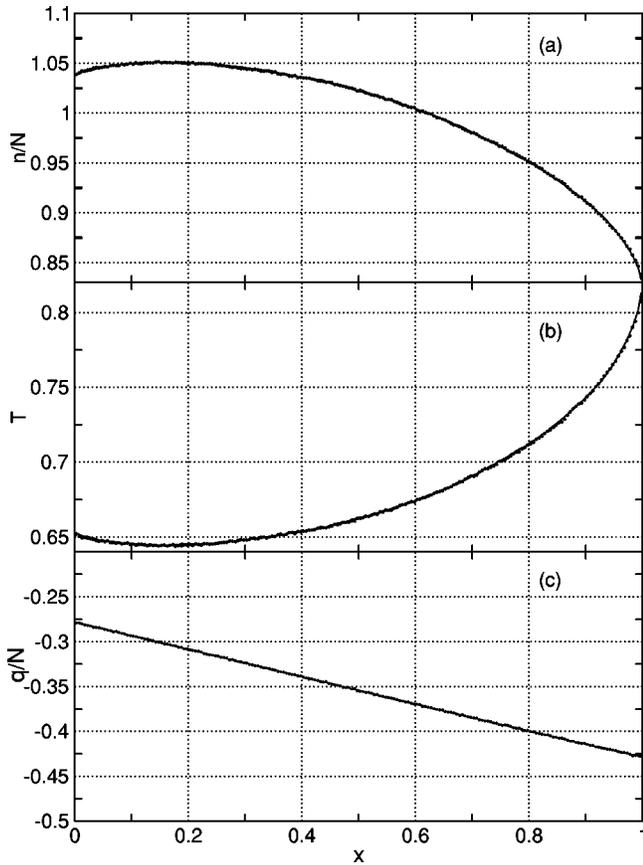
FIG. 4. Number density, temperature, and heat flux profiles for $N=1000$, $qN=0.1$, and $T_{left}=0.5$ ($\Delta=0.6$). The solid line represents results from a molecular dynamics simulation, while the dots represent results from a Monte Carlo simulation. The density and temperature are related by $p=nT$ and, since momentum is conserved and the system is stationary, the pressure is constant throughout the system. The density and temperature profiles are almost symmetrical because the normalized density is very close to unity.
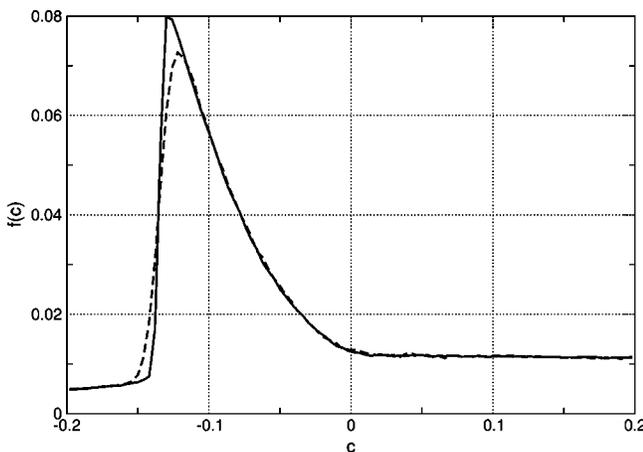
FIG. 5. Velocity distribution function at the cold boundary (left wall) for the system referred to in Fig. 4. The solid line represents results from a molecular dynamics simulation, while the dashed line represents results from a Monte Carlo simulation.
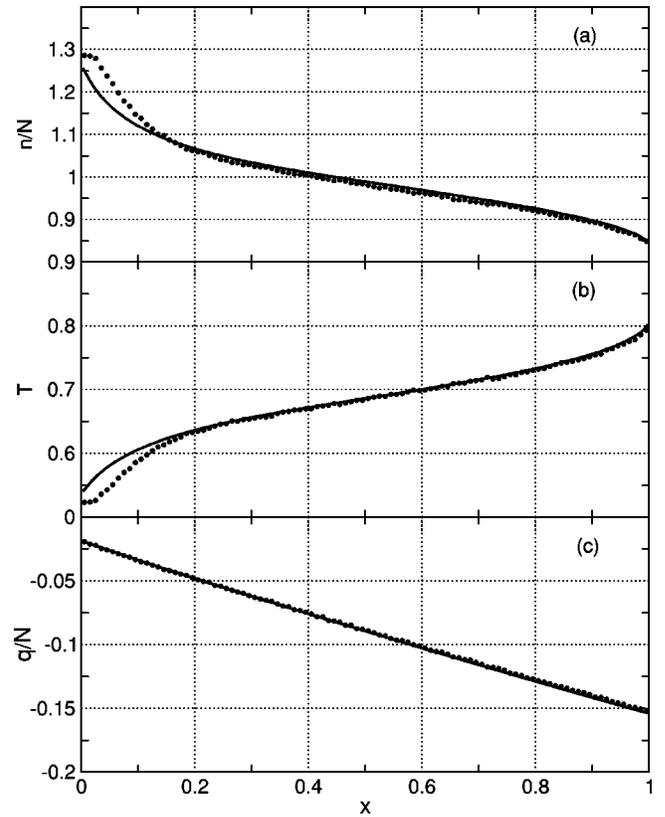
FIG. 6. Number density, temperature, and heat flux profiles for $N=1000$, $qN=0.1$, and $T_{left}=0.84$ ($\Delta=0.173$). The solid line represents results from a molecular dynamics simulation, while the dots represent results from a Monte Carlo simulation.

simulations: there is overpopulation for slow velocities. This is explained by considering that the DSMC method, like the Boltzmann equation, neglects correlations. When the system approaches the clustering regime, increased dissipation induces correlations which tend to make the particles collide less [16]. In DSMC these correlations are neglected, with the corresponding systematic overestimation in the collision frequency. This overestimation results in a lower temperature of the system about the density peak.

IV. CONCLUSIONS

We have shown that a system not subject to gravity between thermal walls unavoidably reaches a nonsteady state when the walls are at the same temperature. A cluster forms in the bulk, slowly roaming about the system while absorbing particles. As it grows, the amplitude of the random walk increases, until at last the surrounding gas cannot keep the cluster away from the walls. When the cluster reaches a wall, a part of it is ejected by the wall *through the cluster* (relabeling the particles on collisions), effectively pushing the cluster away from the wall, and leaving it to grow again.

Most of the time the cluster is far from the walls. Thus measuring the distribution function at a wall is measuring the
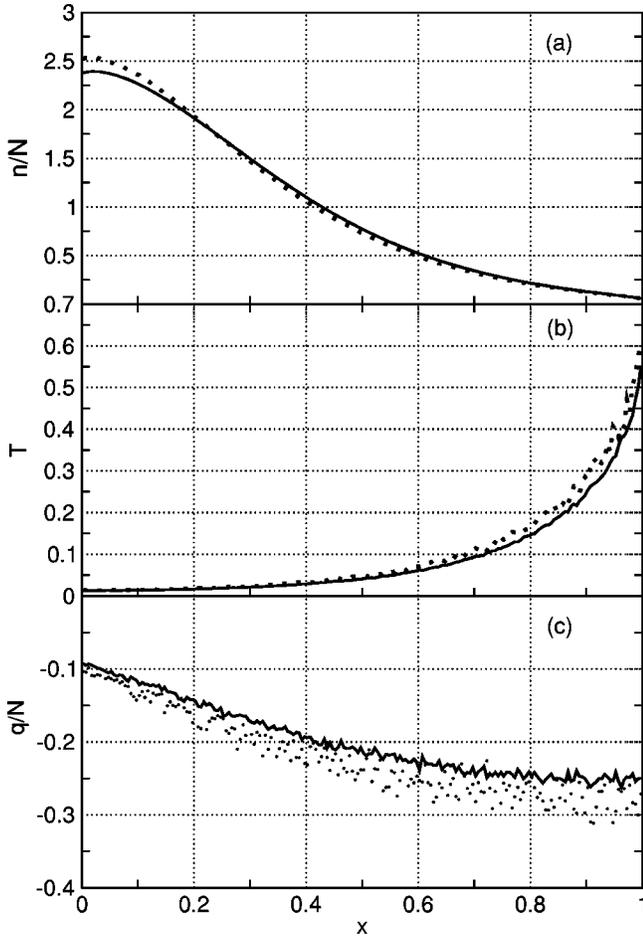
FIG. 7. Number density, temperature, and heat flux profiles for $N=1000$, $qN=0.5$, and $T_{\text{left}}=0.01$ ($\Delta=0.9998$). The solid line represents results from a molecular dynamics simulation, while the dots represent results from a Monte Carlo simulation.

FIG. 8. Velocity distribution functions at the cold boundary (left wall); (a) corresponds to the system referred to in Fig. 6, while (b) corresponds to the system of Fig. 7. The solid line represents results from a molecular dynamics (MD) simulation, while the dashed line represents results from a Monte Carlo (DSMC) simulation. The MD results have been rescaled so that the area under the MD and DSMC curves is the same. There is a systematic overpopulation of slow particles in the distributions obtained from Monte Carlo simulations.

distribution function of the gas that surrounds the cluster. This distribution function has a well-defined time average, and exhibits apparently singular behavior for slow particles, diverging like $|c|^{-1/2}$.

Imposing an external temperature gradient forces the cluster against the colder wall, inhibiting its growth. Increasing the temperature difference leads to a system in which the cluster never forms: the system is completely fluidized. The distribution function of the gas exhibits peculiar non-Gaussian features: a smooth version of the aforementioned singularity. Therefore any attempt at solving the Boltzmann equation through moment methods must consider this feature in the initial ansatz, as is done for the problem of an infinitely strong shock wave in Ref. [25] and [26]. In fact, a solution for this problem was attempted using the four moment method of Ref. [27]. As mentioned in Refs. [28], the fourth balance equation could not be freely chosen when the boundary conditions were symmetric: some choices gave undefined results. As is natural, by not including the non-Gaussian feature in the ansatz for this calculation we obtained absurd results, such as higher temperature in the middle of the system than near the walls.

We compared molecular dynamics with direct-simulation Monte Carlo. Agreement between these two methods shows that the non-Gaussian feature of the distribution function may be predicted by the dissipative Boltzmann equation. As the system approaches cluster formation, correlations settle in. These correlations reduce the collision frequency among particles. DSMC neglects these correlations, and thus overestimates the number of collisions. This exaggerates the effects of dissipation, producing steeper profiles.

[1] L. P. Kadanoff, Rev. Mod. Phys. **71**, 435 (1999).

[2] H. M. Jaeger and S. R. Nagel, Science **255**, 1523 (1992).

[3] H. M. Jaeger, S. R. Nagel, and R. P. Behringer, Phys. Today **49** (4), 32 (1996).

[4] S. McNamara and W. R. Young, Phys. Fluids A **4**, 496 (1992).

[5] S. McNamara and W. R. Young, Phys. Rev. E **50**, R28 (1994).

[6] I. Goldhirsch and G. Zanetti, Phys. Rev. Lett. **70**, 1619 (1993).

[7] A. Kudrolli, M. Wolpert, and J. P. Gollub, Phys. Rev. Lett. **78**, 1383 (1997).

[8] E. Falcon *et al.*, Phys. Rev. Lett. **83**, 440 (1999).

[9] O. Petzschmann *et al.*, Phys. Rev. Lett. **82**, 4819 (1999).

[10] A. Puglisi *et al.*, Phys. Rev. Lett. **81**, 3848 (1998).

[11] A. Puglisi, V. Loreto, U. Marini Bettolo Marconi, and A. Vulpiani, Phys. Rev. E **59**, 5582 (1999).

[12] Y. Du, H. Li, and L. P. Kadanoff, Phys. Rev. Lett. **74**, 1268 (1995).

[13] E. L. Grossman and B. Roman, Phys. Fluids **8**, 3218 (1996).

[14] E. L. Grossman, T. Zhou, and E. Ben-Naim, Phys. Rev. E **55**, 4200 (1997).

[15] T. Zhou, Phys. Rev. Lett. **80**, 3755 (1998).

[16] T. Zhou, Phys. Rev. E **58**, 7587 (1998).

[17] R. Ramírez and P. Cordero, Phys. Rev. E **59**, 656 (1999).

[18] R. Ramírez, D. Risso, and P. Cordero, Phys. Rev. Lett. **85**, 1230 (2000).

[19] T. Biben and J. Piasecki, Phys. Rev. E **59**, 2192 (1999).

[20] S. McNamara and W. R. Young, Phys. Fluids A **5**, 34 (1993).

[21] B. Bernu, F. Delyon, and R. Mazighi, Phys. Rev. E **50**, 4551 (1994).

[22] M. Marín, D. Risso, and P. Cordero, J. Comput. Phys. **109**, 306 (1993).

[23] G. A. Bird, *Molecular Gas Dynamics and the Direct Simulation of Gas Flows* (Clarendon Press, Oxford, 1994).

[24] K. Koura, Phys. Fluids **29**, 3509 (1986).

[25] H. Grad, in *Transport Theory*, edited by R. Bellman, G. Birkhoff, and I. Abu-Shumays (American Mathematical Society, Providence, RI, 1969), pp. 269–308.

[26] C. Cercignani, A. Frezzotti, and P. Grosfils, Phys. Fluids **11**, 2757 (1999).

[27] C. Y. Liu and L. Lees, in *Rarefied Gas Dynamics*, edited by L. Talbot (Academic Press, Berkeley, CA, 1961), pp. 391–428.

[28] P. J. Clause and M. Mareschal, Phys. Rev. A **38**, 4241 (1988).